Archaeological Prospection
Archaeol. Prospect. **21**, 103–112 (2014)
Published online 16 October 2013 in Wiley Online Library
(wileyonlinelibrary.com) DOI: 10.1002/arp.1467

Comparing Apparent Magnetic Susceptibility Measurements of a Multi-receiver EMI Sensor with Topsoil and Profile Magnetic Susceptibility Data over Weak Magnetic Anomalies

PHILIPPE DE SMEDT[1]*, TIMOTHY SAEY[1], EEF MEERSCHMAN[1], JEROEN DE REU[2], WIM DE CLERCQ[2] AND MARC VAN MEIRVENNE[1]

[1] *Research Group Soil Spatial Inventory Techniques, Department of Soil Management, Ghent University, Coupure 653, B-9000, Ghent, Belgium*
[2] *Department of Archaeology, Ghent University, Sint-Pietersnieuwstraat 35, B-9000, Ghent, Belgium*

ABSTRACT Today, most surveys in archaeogeophysical prospection use magnetic properties to detect archaeological features. Such magnetic surveys are usually conducted with magnetometers and, to a lesser extent, with magnetic susceptibility meters and electromagnetic induction (EMI) sensors. Although the latter are the only instruments that allow mapping multiple physical soil properties simultaneously, EMI remains the odd-one-out in archaeogeophysical prospection. Nevertheless, by simultaneously recording the electric and magnetic soil variability, EMI survey can be beneficial in early archaeological evaluation stages, because detailed pedological and archaeological information is gathered at the same time. Furthermore, by using multi-receiver EMI instruments vertical soil variation also can be integrated into the survey. However, although the potential of EMI for mapping electric soil variations is well known from advances in soil science, magnetic susceptibility measurements have been investigated less. Here we show the potential of a multi-receiver EMI survey to detect weak magnetic anomalies by measuring the apparent magnetic susceptibility (κ_a) of multiple soil volumes at a test site. The shallow κ_a data were compared with topsoil susceptibility measurements using a magnetic susceptibility loop sensor survey, and with magnetic susceptibility profiling using a probe sensor for evaluating the deeper κ_a-data. Further comparisons were made between these datasets and aerial photography and field walking data. We found that the multiple EMI κ_a measurements allowed for a straightforward discrimination of the natural and anthropogenic magnetic variations of shallow and deeper soil volumes, and allowed visualizing weak magnetic anomalies. Copyright © 2013 John Wiley & Sons, Ltd.

Key words: Electromagnetic induction; magnetic susceptibility; apparent magnetic susceptibility; multi-receiver EMI; susceptiblity profiling; Bartington MS2

Introduction

Over the past 20 years, the shift from a largely academic framework for archaeological investigations to a developer-led archaeology has resulted in an overwhelming increase in evaluation surveys in western Europe (De Clercq *et al*., 2011). Combined with technological advances and their commercialization, this evolution stimulates the application of geophysical techniques as a standard part of site assessment (Jordan, 2009). However, whereas the archaeological and pedological characteristics of the evaluated sites are seldom alike, the applied geophysical methodologies remain rather uniform. Today, the three main survey techniques are ground-penetrating radar (GPR), electrical resistivity measurements (ER) and magnetometry, which indisputably dominates the archaeogeophysical toolbox (Gaffney, 2008). The almost dogmatic application of magnetometry has pushed the importance of detailed soil mapping to the background, because in these surveys no significant information is gathered

* Correspondence to: P. de Smedt, Research Group Soil Spatial Inventory Techniques, Department of Soil Management, Ghent University, Coupure 653, B-9000 Ghent, Belgium. E-mail: Philippe.DeSmedt@UGent.be

Received 28 January 2013
Accepted 30 September 2013

about the pedology of surveyed sites. Nevertheless, exhaustive mapping techniques are needed that can offer insight into archaeological as well as pedological and geomorphological variations. As geophysical techniques are usually deployed during the first phases of a site evaluation, the incorporation of accurate pedological analyses, or the lack thereof, can have a major impact on the entire research process. Here the application of different methodologies, for example, magnetic and electrical techniques, can offer an outcome by recording straightforward information about natural and anthropological soil variations simultaneously. However, particularly in commercial programmes, multiplying survey runs is not always an option.

The introduction of electromagnetic induction (EMI) instruments with 'Slingram' geometry that enabled recording both the in-phase (IP) and quadrature phase (QP) component of the EMI signal response (e.g. the EM38DD; Geonics, Canada), seemed to offer an efficient solution. While the QP response measures the soil apparent electrical conductivity (σ_a), the IP response is representative for the soil apparent volume magnetic susceptibility (κ_a) (Keller and Frischknecht, 1966). Whereas the σ_a measurements record information about the textural variability, soil organic matter content and moisture content, the κ_a measurements would enable detecting magnetic disturbances comparable with the potential of magnetometry. Unfortunately, the limited penetration depth (Dalan, 2008; Henry, 2011) and difficult interpretation (Simpson *et al*., 2010) of the IP response, combined with the sometimes capricious calibration procedures of these instruments before each survey, have made EMI survey a rare first choice in archaeological evaluations.

In soil science and exploration geophysics the application of EMI instruments persisted (e.g. Fraser, 1972; Slavich and Petterson, 1990; Abdu *et al*., 2007), and stimulated the development of new and more integrated types of EMI systems. The introduction of multi-receiver instruments that allow measuring the σ_a and κ_a of different soil volumes (e.g. Dualem-21S, Geonics MK-2) has renewed the potential of EMI surveys in archaeology. These instruments combine a transmitter coil with multiple receiver coils, which are placed at different, but fixed, distances and often in different orientations. The most frequently used coil orientations are vertical coplanar (VCP), horizontal coplanar (HCP) or perpendicular (PRP) (Reynolds, 1997). Together with the separation between the transmitter and the receiver coils, these different coil orientations influence the depth response of the EMI signal (Keller and Frischknecht, 1966; Butler, 2005).

In recent years, a number of studies have proven the effectiveness of such instruments in recording detailed σ_a variations and detecting archaeological anomalies. In particular, the depth information added by the multiple coil pairs, now allowing the simultaneous recording of up to six different soil volumes (e.g. with the Dualem-421S), has increased the interpretative value of these surveys for archaeological and palaeotopographical studies (Saey *et al*., 2008; Simpson *et al*., 2009; De Smedt *et al*., 2011). The combined analyses of σ_a and κ_a of multi-receiver EMI sensors now allows composing integral reconstructions of human environments, taking into account both the past natural and anthropological variations (e.g. De Smedt *et al*., 2013). However, the main aim of these studies has been on combining and analysing the multiple σ_a measurements. Even though ground-breaking work has been conducted on the use of Slingram EMI sensors for mapping magnetic anomalies (e.g. Tabbagh, 1984, 1986a; Benech and Marmet, 1999), and on the comparison between different magnetic survey techniques (Cole *et al*., 1995; Linford, 1998), the added value of multiple κ_a measurements has been investigated less. Here we show the potential of measuring κ_a of multiple soil volumes simultaneously with a multi-receiver EMI sensor to detect weak magnetic anomalies. Aerial photography, extensive field walking, additional magnetic susceptibility surveying and coring were used to further evaluate the κ_a data. Apart from evaluating the lateral discrimination potential of the κ_a measurements in archaeological surveying, the added value of multiple measurements with different penetration depths for vertical data analysis is discussed.

Study site and non-invasive surveying

Within the framework of a research project aimed at developing a methodology to characterize Roman and medieval rural settlement patterns, a research area of approximately 50 ha was selected in the northwestern part of Belgium. The soil in the area consists of Eocene marine clay overlain by Pleistocene aeolian sand deposits, which often are only a few decimetres thick. At the study site, the topsoil texture has a sand content of about 80% while the underlying layers consist of some 65% clay (Saey *et al*., 2013). A central part of about 3 ha, with a high density of archaeological crop marks (Figure 1A), was selected as a test site to evaluate the use of different non-invasive survey methods. In a first phase, EMI and magnetometry survey were compared with aerial photography data (see De Clercq *et al*. (2012) for further information) (Figure 1A–D). In addition to geophysical survey, extensive aerial photography prospection has been

DOI: 10.1002/arp

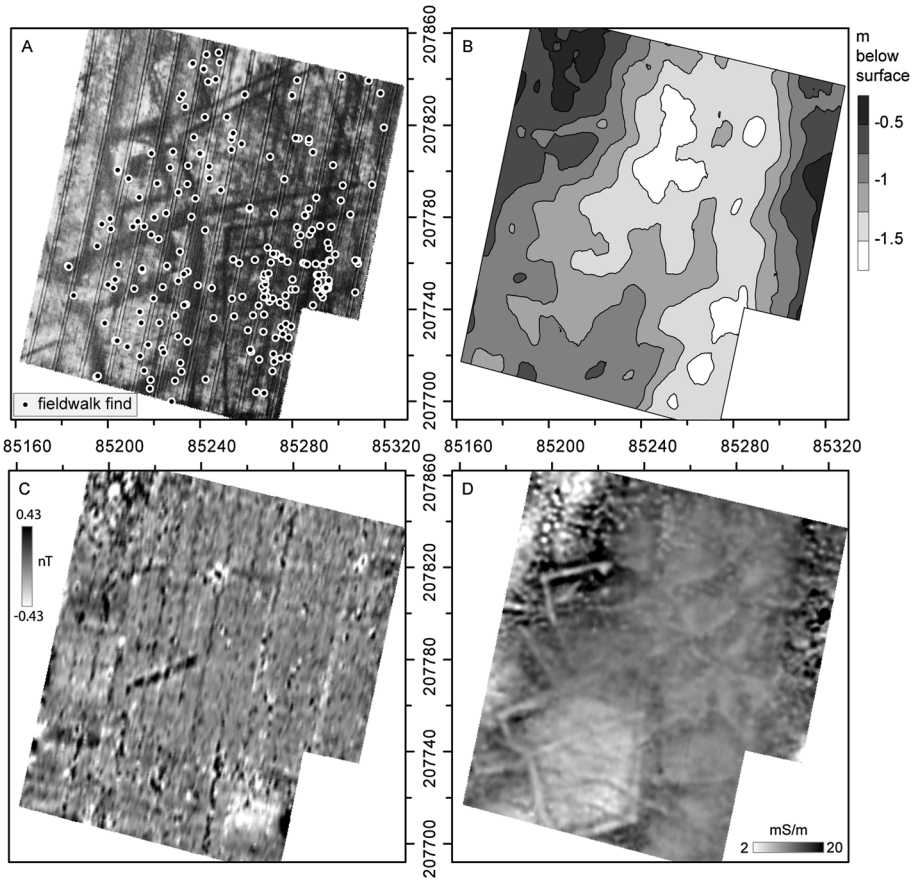

Figure 1. (A) Aerial orthophotograph of the study field (aerial photograph 553546, taken on 4 June 2010, Department of Archaeology, Ghent University) with field-walk finds indicated. (B) Palaeotopography of the site: depth to the Eocene clay below the sand (Saey *et al*., 2013). (C) Fluxgate gradiometer data (source: P. Masters – De Clercq *et al*., 2012). (D) Electrical conductivity depth slice resulting with removal of the interference of the underlying palaeotopography (Saey *et al*., 2013).

conducted, along with two field-walking campaigns (1.5 m between survey lines). As the multi-receiver EMI survey showed that the average σ_a of the test site was relatively high (57 mS m^{-1} for the 1 m HCP coil configuration and 88 mS m^{-1} for the 2 m HCP coil configuration), the required conditions for effective EMI surveying – a σ_a between 1 and 100 mS m^{-1} – were met (McNeill, 1980; Callegary *et al*., 2007), indicating that the IP and QP signal components should accurately represent κ_a and σ_a variations, respectively. The σ_a data revealed a large number of archaeological features, which could be related to the enclosures in the western and southwestern part of the field. After implementing a two-step inverse modelling of the four conductivity data to obtain depth slices (Saey *et al*., 2013), additional small-scale linear features could be discerned that did not appear in the aerial photography or magnetometry dataset (Figure 1D). However, a thorough validation and interpretation of these features through test pitting and coring still needs to be performed. Apart from the large amount of archaeological features of the site, the EMI survey revealed a significant palaeotopographical variation, which was instrumental as to the choice of settlement location. Through inversion of the EMI conductivity data, following the inversion procedure of Saey *et al*. (2008), a reconstruction was made of the depth to the Eocene clay (Saey *et al*., 2013). In the northern and central parts of the test site a depression was found in the Eocene clay, which was filled up with a layer of aeolian Pleistocene sand 1.5 m thick (Figure 1B).

Measurements of κ_a with a multi-receiver EMI sensor

The EMI survey was conducted with a Dualem 21-S sensor (Dualem, Canada), which combines one transmitter coil (*T*) with four receiver coils (*R*). Two of the receiver coils are placed in perpendicular (PRP)

DOI: 10.1002/arp

orientation at 1.1 m and 2.1 m from *T*, while the remaining receivers are in horizontal coplanar (HCP) orientation at 1 m and 2 m from *T* (Simpson *et al*., 2009). Measurements were taken along parallel lines 0.75 m apart with an in-line sampling resolution of ca. 0.25 m (Table 1). The κ_a values, expressed in dimensionless magnetic susceptibility units (msu), were calculated from the IP response following McNeill and Bosnar (1998): $\kappa_a = 2 \times [0.0001 \times (H_s/H_p)IP]$, with $(H_s/H_p)IP$ the ratio of the in-phase component of the secondary magnetic field to the primary magnetic field. The ratio of the secondary to the primary magnetic field is then multiplied by two in order to account for measuring a half-space (i.e. the soil being one half of the space and the air being the other). All data were drift corrected following Simpson *et al*. (2009). Herein, in the first stage of the survey, a W-shaped reference line was driven across the field. As measurements conducted along this line are taken directly after sensor start-up, it can be assumed that the absolute observed κ_a and σ_a are correct. Each subsequent survey line was then driven across this reference line. During processing, the individual survey lines were then compared with the reference line. The differences between the κ_a and σ_a values measured along the reference line and those on the subsequent survey lines within a distance of 3 m from the nearest reference measurement were then compared in order to estimate the influence of drift on each survey line. Afterwards results were interpolated to a 0.1 × 0.1 m grid through ordinary kriging in Surfer (Golden Software).

For the IP signals of the Dualem 21-S coil pairs, the cumulative depth responses vary from approximately 1 m to 1.5 m below the sensor for the HCP coil pairs, and from 0.6 m to 1.2 m below the sensor for the PRP coil pairs, based on the theoretical response functions and experimental observations. These soil volumes encompass the depth range of archaeological features in most archaeological surveys (exceptions include sedimentation areas where thick layers of, for example alluvial, deposits cover archaeological features). Furthermore, a multivolume survey enables differentiating between topsoil κ_a and the κ_a of deeper soil layers.

There are still a number of limitations inherent to the HCP and PRP coil configurations. Whereas HCP coil pairs enable very stable IP measurements, the cumulative response of these configurations has a signal change below a certain depth (Tabbagh, 1986b) (Figure 2). As a consequence, highly magnetic anomalies that are below this critical depth, but still fall within the detectable range of the coil pair, appear as anomalies with a reduced κ_a within the surrounding area and *vice versa* (Simpson *et al*., 2010). This can hamper a straightforward interpretation of IP data collected with a HCP coil pair. When using a single receiver EMI instrument with HCP coil geometry, without knowledge of the depth of a detected feature, it can be difficult to interpret whether the anomaly is highly magnetic or has a lower susceptibility than the surrounding soil. For the Dualem-21S sensor, this critical depth is approximately 0.6 m for the 1 m HCP coil pair (D1 on Figure 2) and 1.2 m for the 2 m HCP coil pair (D2 on Figure 2). In PRP orientation, the IP response suffers less from signal change, but in field conditions these measurements are often unstable, which makes them less suited for visualizing archaeological features. For example, when the magnetic contrast between features is low or in environments with considerable magnetic background variability (such as heterogeneous soil mineralogy or the presence

Table 1. Sample density for the EMI survey, the Bartington MS2D loop sensor survey and the magnetometry survey (see Figure 1C and De Clercq *et al*., 2012).

	Dualem 21-S	Bartington MS2D	Magnetometry
Sample density	0.75 m × ca. 0.25 m	10 m × 10 m	0.25 m × 1 m

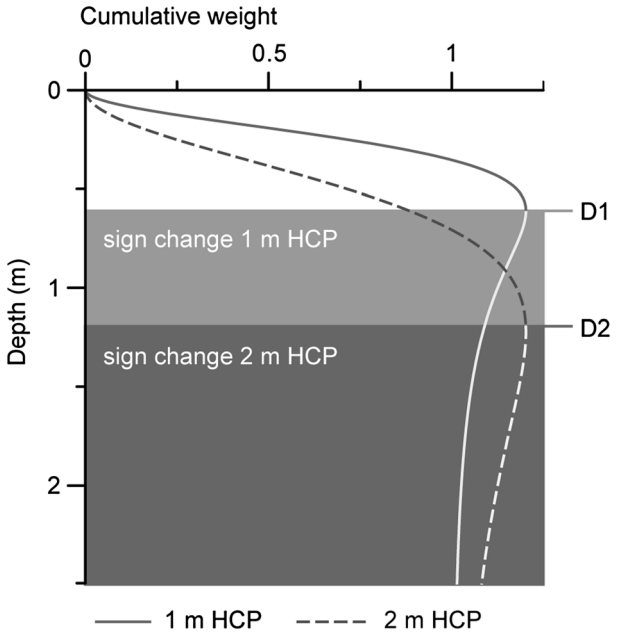

Figure 2. Cumulative depth responses of in-phase response of the 1 m and 2 m HCP coil pairs. D1 and D2 represent the critical depth for the 1 m and 2 m HCP configuration respectively, where the signal response inverses. The dark part of the curves represents the positive response and the white part represents the inverted or negative response.

DOI: 10.1002/arp

of ferrous utility pipes) the interpretation of the PRP IP response can be hampered by instrument-induced noise.

At the test site, the PRP data suffered from a poor signal to noise ratio. Apart from a number of linear features that could be attributed to recent agricultural activities, interpretation of all PRP datasets was hindered by the distinct 'salt-and-pepper' noise (Figure 3A). Results for the 1 m and 2 m HCP coil configurations (Figure 3B and C), on the other hand, showed the discrimination potential of the EMI κ_a measurements. While the magnetometry results did not allow for reconstructing the layout of the site (Figure 1C) (De Clercq *et al.*, 2012), with EMI two large enclosures could be discerned on the 1 m HCP κ_a data, along with a number of pits and ditches. However, a discrepancy remained between the geophysical results and the aerial photographs, as nearly 50% of the archaeological features seen from the air did not show up in the magnetometry or the κ_a data. A similar difference could be observed between the κ_a and the sliced σ_a data (Figure 1D). The subtle linear features discriminated in the electrical conductivity slice in the central and eastern part of the field did not appear in any of the κ_a data layers. In the 2 m HCP κ_a data, only few archaeological traces were visible, indicating the shallow depth extent of the features. Here, more background variation was observed, coinciding with the pedological variation witnessed in the σ_a measurements. Apart from the apparently deeper parts of the detected enclosures, the detected magnetic anomalies were weak, rendering a maximum κ_a of 0.0016 msu for the 1 m HCP coil pair and of 0.0041 msu for the 2 m HCP coil pair in the EMI data.

Magnetic susceptibility measurements with the Bartington MS2 system

To complement the EMI-derived κ_a data, and to account for differences between these and other available survey data, a Bartington MS2 magnetic susceptibility system was used coupled to a MS2H subsurface probe and a MS2D loop sensor. The MS2 sensors operate on the principle of frequency domain EMI, which is similar to Slingram EMI instruments. However, the MS2 measurements have the advantage that these are fairly insensitive to the electrical conductivity of the measured medium, whereas in certain conditions, for example in saline environments, the κ_a or IP response of an EMI sensor can be influenced by the soil electrical conductivity or QP response

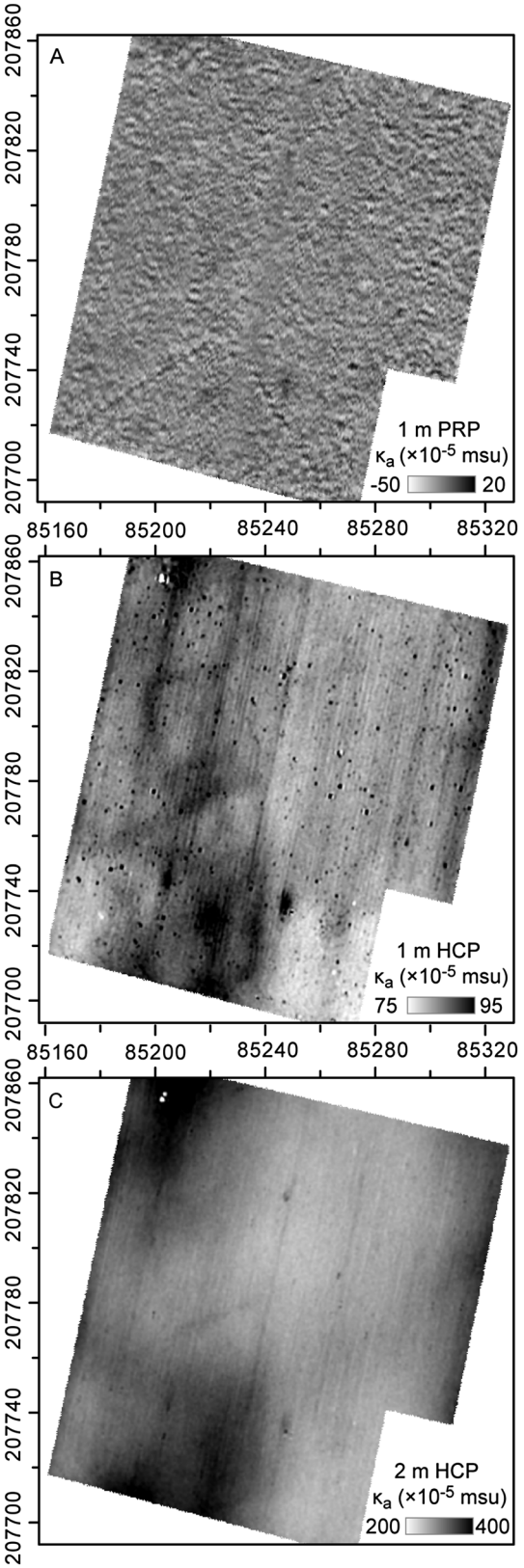

Figure 3. The κ_a data (interpolated to a 0.1 m × 0.1 m grid) from the 1 m PRP (A), 1 m HCP (B) and 2 m HCP (C) coil configurations.

DOI: 10.1002/arp

(Callegary *et al*., 2007). This way, the MS2 sensors can be used to evaluate the possible interference between IP and QP signal components of EMI measurements. Note that in this paper we discriminate between apparent magnetic susceptibility measurements (κ_a) from the EMI sensor and the Bartington MS2D loop sensor, and true magnetic susceptibility (κ) data from the Bartington MS2H probe, whereby we omit the prefix 'apparent' (i.e. the subscript 'a').

In a first step, topsoil κ_a was measured with the MS2D loop sensor. The effective penetration depth of the MS2D, which corresponds to 90% of the recorded signal, is considered to be 6 cm (Lecoanet *et al*., 1999), whereby 50% of the signal response is obtained at 1.5 cm below the sensor, as described in the Bartington instrument specifications. In total, 225 measurements were taken in a 10 m by 10 m grid (Table 1) with the 1.0 measurement range, that is, an accuracy of 1×10^{-5} SI units, whereby the instrument was zeroed before each measurement. These measurements were then interpolated to a 2.5 m × 2.5 m grid using ordinary kriging (Goovaerts, 1997). Apart from a general comparison between the MS2D data and the EMI survey, we wanted to evaluate the analogy between the spatial κ_a variations detected with the MS2D measurements and the EMI κ_a data.

To investigate the relationship between the subsurface features and geophysical data further, 15 locations were selected for κ profiling with the MS2H probe. The MS2H probe has a 0.5 cm horizontal signal-depth penetration around its tip and a vertical resolution of 1.25 cm (Bartington instrument specifications). At each location, a borehole was prepared with a 2.5 cm gouge auger and lithological descriptions were made. The κ measurements were taken at 5 cm intervals, starting at a depth of 10 cm, down to at least 50 cm depending on the position of the undisturbed substrate. Along with the κ measurements, the lithology of the profiles was described. To allow a straightforward comparison of the different measurements, all κ and κ_a data are represented in the 1×10^{-5} range.

Topsoil magnetic susceptibility: MS2D

The MS2D measurements were compared with the 1 m HCP Dualem-21S data (Figure 4A, B), as the latter are influenced more by topsoil variations than the 2 m HCP measurements. The difference in measured soil volume between both datasets results in a mean κ for the MS2D data that is nearly ten times lower than the results from the 1 m HCP κ_a measurements (Table 2): this can be explained by the larger soil volume that is taken into account in the 1 m HCP measurements.

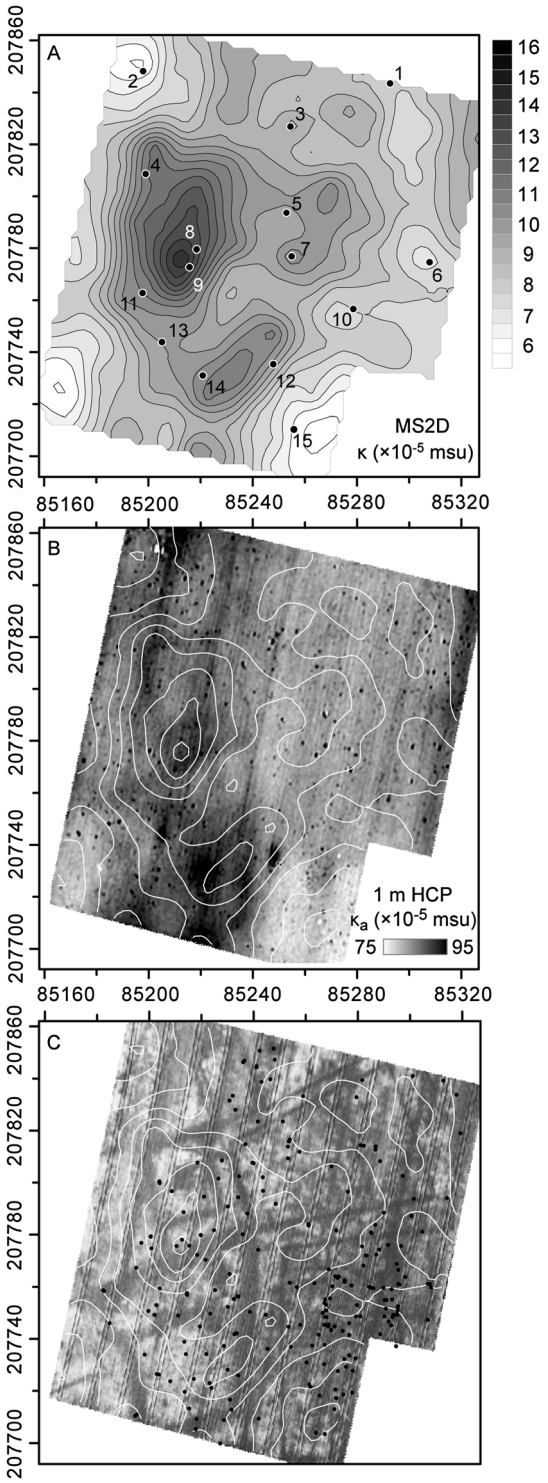

Figure 4. The κ_a data from the MS2D survey (interpolated to a 2.5 m × 2.5 m grid) with (A) the MS2H probing and coring locations, (B) major MS2D κ_a data contours plotted on the 1 m HCP κ_a measurements (Figure 3B) and (C) major MS2D κ_a data contours and field-walking finds (dots) plotted on the aerial orthophotograph (Figure 1A).

DOI: 10.1002/arp

Table 2. Descriptive statistics of the different κ_a measurements.

Statistic	Dualem 21-S		Bartington MS2	
	1 m HCP	2 m HCP	MS2D	MS2H
Average	86	315	9	9
Minimum	29	130	4	0
Maximum	185	452	17.9	34*
Standard deviation	5	25	2	13

The κ_a values are expressed in 1×10^{-5} msu SI
*(excluding one outlier of 160×10^{-5} msu for profile 6).

However, the standard deviations of both datasets lie more closely together and vary only 3×10^{-5} msu, indicating that whereas the MS2D survey resulted in a broad data range, the 1 m HCP κ_a measurements are closely clustered around the mean. Again, this can be attributed to the volumetric difference between both survey datasets. The shallow depth penetration of the loop sensor gives a high local resolution, whereas the 1 m HCP coil pair takes into account a much larger soil volume, which has a smoothing effect on the individual measurements. As a result, each measurement is slightly smoothed by taking into account more of the background variation within the measured soil volume. In other words, the MS2D offers sharper κ_a contrasts than the 1 m HCP data.

A similar spatial trend could be observed between the MS2D and the 1 m HCP κ_a data (Figure 4B); most of the magnetic variation is present in the south to southwestern part of the field. In the MS2D data, the most dominant magnetic anomaly was detected around the small enclosure. On the other hand, the most southern and largest enclosure had a smaller influence on the measurements than observed in the 1 m HCP data. In the northeastern part of the field, a larger κ_a variation was attested in the MS2D dataset. This could indicate that the archaeological features seen on the aerial photograph in this part of the field represent very shallow magnetic anomalies.

To evaluate the potential of the MS2D to detect the spread of archaeological activity areas, these data were compared with the aerial-photograph and the field-walking results (Figure 4C). Most of the assembled finds are located within the enclosures seen on the aerial photograph. Still, the correlation between the field-walking data and the MS2D results remains the strongest for the enclosures that can also be discerned in the EMI data. The spatial distribution of the finds in the eastern and southeastern part of the field shows a different pattern than observed in the MS2D plot. This was most apparent in the southeastern part of the field where the highest concentration of surface material was found, but no enhanced κ_a could be detected with the MS2D loop sensor.

Magnetic susceptibility profiling: MS2H

The MS2H profiles showed that, in general, the more magnetic plough layer had the strongest influence on the κ measurements, with an average of 16.7×10^{-5} msu (Figure 5). However, only at four locations (8, 9, 12 and 13 on Figure 4A and Figure 5) was an unusual increase of κ attested in the plough layer, coinciding with observed magnetic variations at these locations in the 1 m HCP and MS2D data.

The average κ of the deeper layers was 4.6×10^{-5} msu. Here, a distinction could be made between the susceptibility of the undisturbed soil and the archaeological layers. At nine locations (1, 3, 4, 8, 9, 10, 11, 13 and 14) black organic-rich sand was present, often with traces of brick, burnt material and oxidation, which was identified as an archaeological layer. However, only in a few cases a slight increase in κ was observed in this layer (locations 4, 8, 9, 11 and 14). At these locations, the enhanced susceptibility of the archaeological layer was also observed in the 2 m HCP κ_a measurements, showing the potential of the deeper EMI measurements to discriminate small variations in κ_a.

The MS2H profiles further showed a significant contribution of the undisturbed soil to the overall κ of the site. Whereas the sand and sandy clay layers had a generally low κ value (between 0 and 1×10^{-5} msu), the mineralogy of the Eocene clay caused a significant increase in κ (mainly between 1 and 2×10^{-5} msu). Only at one location did a ferrous horizon cause higher κ in the sand (profile 5 on Figure 5). This increased κ of the Eocene clay was also attested in the 2 m HCP measurements where, particularly in the northwestern, eastern and southwestern part of the field, large areas with increased κ_a were observed. The contribution of the Eocene clay to the 2 m HCP κ_a measurements was most clearly attested at location 2, where the depth to the clay layer was only 40 cm. However, at locations 9, 11 and 13 the contribution of the Eocene clay to the 2 m HCP data was negligible. Here, the depth to clay was below 120 cm, that is, below the critical depth of the 2 m HCP coil configuration for detecting κ variations, and only more shallow features could be discriminated. As an example we refer to location 9 where the 2 m HCP measurements allowed discrimination of the elevated κ of the archaeological layer, but influence from the underlying clay layer could not be observed.

DOI: 10.1002/arp

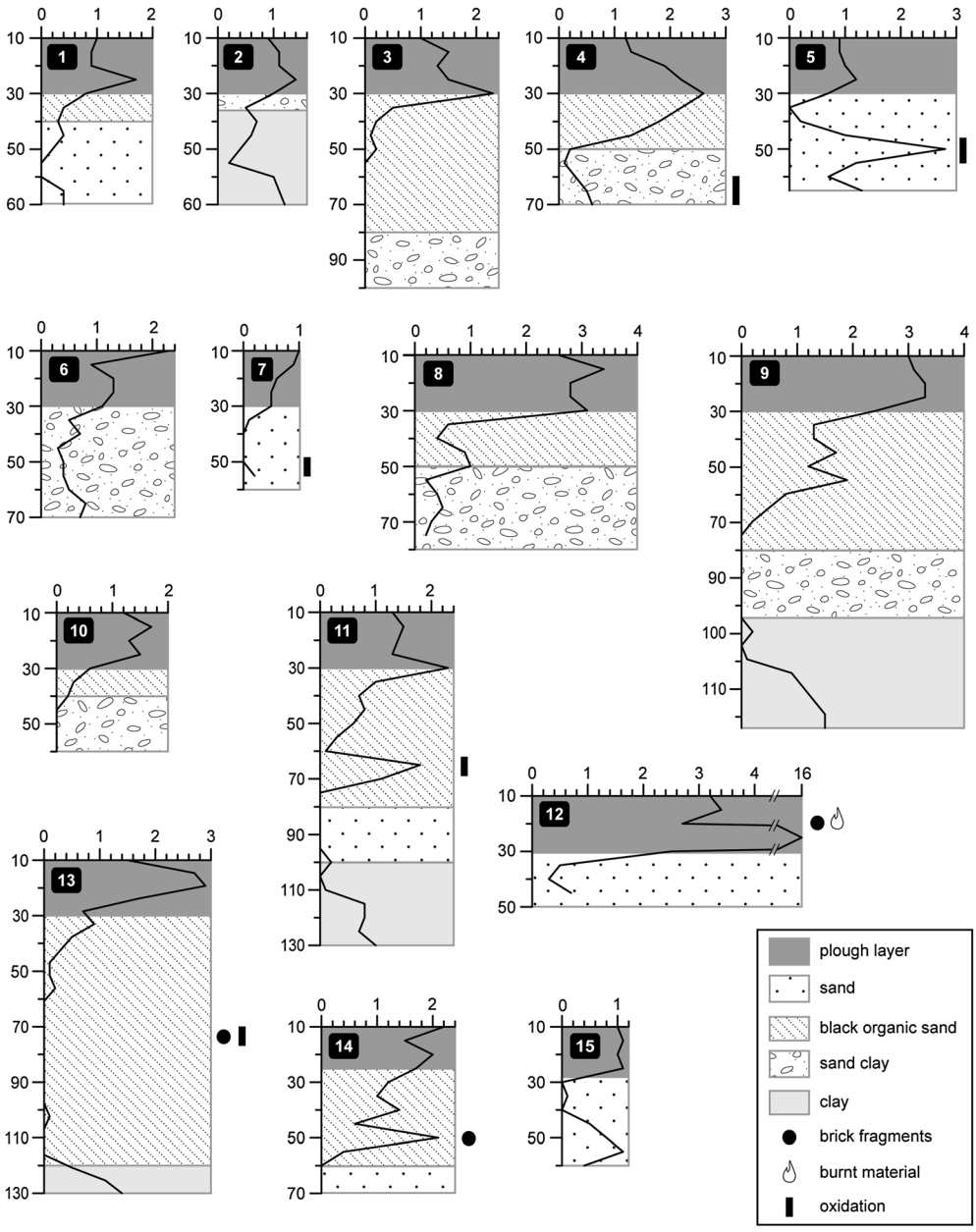

Figure 5. The MS2H κ profiles with the observed stratigraphy indicated. *X* axis: κ ($\times 10^{-4}$ msu); *Y* axis: depth in centimetres.

Discussion and conclusion

Overall the κ profiles show that where archaeological layers were encountered, the susceptibility of the plough layer increased significantly (i.e. between 1 and 2×10^{-5} msu instead of $> 1 \times 10^{-5}$ msu where no archaeological features were detected). The resulting enhanced topsoil susceptibility caused the variations that were detected with the MS2D survey. In nearly all cases this variation was recorded in the 1 m HCP κ_a measurements, only at locations 1 and 3 were the slight κ increases not reflected in the EMI data. The 2 m HCP measurements were also proven to be representative for the elevated κ of the archaeological layer for depths surpassing 50 cm below the surface. In addition, κ profiling allowed correlating the large-scale κ trend observed in the 2 m HCP data to the higher susceptibility of the clay layer. Combined with comparison with the observed σ_a variations at the site, this shows the independence of the IP response of

DOI: 10.1002/arp

the HCP coil configurations of the soil conductivity or QP signal response.

Through comparing different measurements of soil κ we have gained a clearer insight into the influence of archaeological and pedological features on multi-receiver EMI κ_a measurements. Even when the archaeological features displayed only a small contrast in κ, it was possible to clearly discriminate such features in the EMI κ_a data. Furthermore, the integration of multiple simultaneous κ_a measurements of different soil volumes allows accurate discrimination between topsoil κ and magnetic variations of deeper soil layers.

Acknowledgements

The authors would like to thank dr ir Bruno De Vos from the Research Institute for Nature and Forest (INBO) – Environment and Climate Unit – for lending us the MS2D loop sensor. We are grateful to dr Birger Stichelbaut for providing detailed information on the aerial photograph. We also thank farmers Gabriel and Filip Landuyt for granting us unlimited access to the test site, and thank dr Ludovic Letourneur from Bartington Instruments for the interesting discussions on the Bartington MS2 sensor equipment.

References

Abdu H, Robinson DA, Jones SB. 2007. Comparing bulk soil electrical conductivity determination using the DUALEM-1S and EM38-DD electromagnetic induction instruments. *Soil Science Society of America Journal* **71**(1): 189–196.

Benech C, Marmet E. 1999. Optimum depth of investigation and conductivity response rejection of the different electromagnetic devices measuring apparent magnetic susceptibility. *Archaeological Prospection* **6**(1): 31–45.

Butler DK. (ed.). 2005. *Near-surface Geophysics. Investigations in Geophysics*. Society of Exploration Geophysicists: Tulsa, OK.

Callegary JB, Ferre TPA, Groom RW. 2007. Vertical spatial sensitivity and exploration depth of low-induction-number electromagnetic-induction instruments. *Vadose Zone Journal* **6**(1): 158–167.

Cole MA, Lindford N, Payne A, Linford P. 1995. Soil magnetic susceptibility measurements and their application to archaeological site investigation. In *Science and Site: Evaluation and Conservation*, Beavis J, Barker K (eds). Bournemouth University: Bournemouth; 114–162.

Dalan RA. 2008. A review of the role of magnetic susceptibility in archaeogeophysical studies in the USA: recent developments and prospects. *Archaeological Prospection* **15**(1): 1–31.

De Clercq W, Bats M, Laloo P, Sergant J, Crombé P. 2011. Beware of the known. Methodological issues in the detection of low density rural occupation in large-surface archaeological landscape-assessment in Northern-Flanders (Belgium). In *Understanding the Past: a Matter of Surface-area. Acts of the XIIIth Session of the EAA congress, Zadar 2007*, Blanquaert G, Malain F, Stäube H, Vanmoerkerke J (eds). British Archaeological Reports, International Series. Archaeopress: Oxford; 73–89.

De Clercq W, De Smedt P, De Reu J, *et al*. 2012. Towards an integrated methodology for assessing rural settlement landscapes in the Belgian Lowlands. *Archaeological Prospection* **1**(2): 141–145.

De Smedt P, Van Meirvenne M, Meerschman E, *et al*. 2011. Reconstructing palaeochannel morphology with a mobile multicoil electromagnetic induction sensor. *Geomorphology* **130**(3–4): 136–141.

De Smedt P, Van Meirvenne M, Herremans D, *et al*. 2013. The 3-D reconstruction of medieval wetland reclamation through electromagnetic induction survey. *Scientific Reports* **3**(1517): 5 pp.

Fraser D. 1972. A new multicoil aerial electromagnetic prospecting system. *Geophysics* **37**(3): 518–537.

Gaffney C. 2008. Detecting trends in the prediction of the buried past: a review of geophysical techniques in archaeology. *Archaeometry* **50**(2): 313–336.

Goovaerts P. 1997. *Geostatistics for Natural Resources Evaluation*. Applied Geostatistics Series. Oxford University Press: New York.

Henry ER. 2011. A multistage geophysical approach to detecting and interpreting archaeological features at the LeBus Circle, Bourbon County, Kentucky. *Archaeological Prospection* **18**(4): 231–244.

Jordan D. 2009. How effective is geophysical survey? A regional review. *Archaeological Prospection* **16**: 77–90.

Keller GV, Frischknecht FC. 1966. *Electrical Methods in Geophysical Prospection*. International Series of Monographs in Electromagnetic Waves Volume **10**. Pergamon Press: London.

Lecoanet H, Lévêque F, Segura S. 1999. Magnetic susceptibility in environmental applications: comparison of field probes. *Physics of the Earth and Planetary Interiors* **115**: 191–204.

Linford NT. 1998. Geophysical survey at Bodem Vean Cornwall, including an assessment of the microgravity technique for the location of suspected archaeological void features. *Archaeometry* **40**(1): 187–216.

McNeill JD. 1980. *Electromagnetic terrain conductivity measurement at low induction numbers*. Technical Note 6, Geonics Limited: Ontario.

McNeill JD, Bosnar M. 1998. *Application of dipole-dipole electromagnetic systems for geological depth sounding*. Technical Note 31, Geonics Limited: Ontario.

Reynolds JM. 1997. *An Introduction to Applied and Environmental Geophysics*. J. Wiley & Sons, Inc.: New York.

Saey T, Simpson D, Vitharana UWA, Vermeersch H, Vermang J, Van Meirvenne M. 2008. Reconstrucing the paleotopography beneath the loess cover with the aid of an electromagnetic induction sensor. *Catena* **74**(1): 58–64.

Saey T, De Smedt P, De Clercq W, Meerschman E, Islam MM, Van Meirvenne M. 2013. Identifying soil patterns at different spatial scales with a multi-receiver EMI sensor. *Soil Science Society of America Journal* **77**(2): 382–390.

Simpson D, Van Meirvenne M, Saey T, *et al*. 2009. Evaluating the multiple coil configurations of the EM38DD

DOI: 10.1002/arp

and DUALEM-21S sensors to detect archaeological anomalies. *Archaeological Prospection* **16**(2): 91–102.
Simpson D, Van Meirvenne M, Lück E, Rühlmann J, Saey T, Bourgeois J. 2010. Sensitivity of multi-coil frequency domain electromagnetic induction sensors to map soil magnetic susceptibility. *European Journal of Soil Science* **61**(4): 469–478.
Slavich P, Petterson G. 1990. Estimating average rootzone salinity from electromagnetic induction (EM-38) measurements. *Australian Journal of Soil Research* **28**(3): 453–463.
Tabbagh A. 1984. On the comparison between magnetic and electromagnetic prospection methods for magnetic features detection. *Archaeometry* **26**(2): 171–182.
Tabbagh A. 1986a. Applications and advantages of the Slingram electromagnetic method for archaeological prospecting. *Geophysics* **51**(3): 576–584.
Tabbagh A. 1986b. What is the best coil orientation in the Slingram electromagnetic prospecting method? *Archaeometry* **28**(2): 185–196.

DOI: 10.1002/arp